Anomalous peak in the spectrum of polarizational bremsstrahlung from relativistic electrons moving through a solid target

V Astapenko[1], N Nasonov[2] and P Zhukova[2]

[1] Moscow Institute of Physics and Technology, Dolgoprudnyi, Moscow Region, 141700, Russia
[2] Laboratory of Radiation Physics, Belgorod State University, 14 Studencheskaya st., 308007 Belgorod, Russia

E-mail: nnn@bsu.edu.ru

Received 8 October 2006, in final form 11 January 2007
Published 9 March 2007
Online at stacks.iop.org/JPhysB/40/1337

Abstract

The spectral-angular distribution of polarizational bremsstrahlung from relativistic electrons crossing a polycrystalline target is studied theoretically. The effect of substantial growth in the emission spectral density is predicted for photons emitted in the backward direction relative to emitting electron velocity.

1. Introduction

Polarizational bremsstrahlung (PB) appears in the process of a fast charged particle collision with an atom due to the scattering of the particle Coulomb field by atomic electrons [1–3]. This emission mechanism, additional to ordinary bremsstrahlung, is well studied, as applied to a projectile interaction with an isolated atom (see, for example, the full relativistic description of the total bremsstrahlung including PB given in [4, 5]). On the other hand, PB from a fast particle moving through a solid target has not been adequately explored. The influence of both self-absorption of emitted PB photons [2, 6] and the density effect [1, 7] has been considered recently. In addition to this PB generated in the processes of electron fullerene and electron metal cluster collisions has been studied [2, 8–11]. The last effect caused by the excitation of collective oscillations of delocalized electrons of the target manifests in the range of small photon energies close to plasmon resonance. An important role of collective contributions of the target atoms to the formation of PB yield from dense media in a wide frequency range is caused by the characteristic property of the emission mechanism being discussed, consisting of a large value of an effective PB impact parameter comparable with the atomic size [12]. Collective effects in PB are substantial even for amorphous targets [13, 14], but the role of such effects comes into particular prominence in the case of ordered or partially ordered targets.

Polarizational bremsstrahlung from relativistic electrons moving in a solid target considered as an ordinary polycrystal (it is well to bear in mind that most parts of solid

samples possess a polycrystalline structure) is the subject for study in this paper. The task being considered is of interest in the context of the main distinctive property of PB from a polycrystal as compared with that from an amorphous target. This property consists of the strong suppression of individual contributions of the target's atoms to the PB yield, so that spectral and angular characteristics of PB are determined in the main by the collective contribution of all atoms [12]. By contrast, the ordinary bremsstrahlung from relativistic electrons moving through a polycrystal is formed practically by individual contributions of atoms [15]. The outlined sharp distinction is caused by the difference between effective impact parameters for PB and for bremsstrahlung. In accordance with the theoretical description of PB from relativistic electrons moving in a polycrystal the emission spectrum in the case being discussed contains strong maxima, the position of which is determined by the value of the observation angle [12]. The spectrum of PB from a polycrystal in the frequency range outside the above maxima is strongly suppressed relative to that from an amorphous target [12]. It is significant that the outlined features of PB from a polycrystal were observed experimentally [16, 17]. A good quantitative agreement of data measured recently in experiments with Al, Cu and Ni thin films and 7 MeV electron beam with theoretical predictions has been obtained in the last work devoted to experimental studies of the problem under discussion [18].

The purpose of our study is to show that the above maxima can increase many times under special conditions of emitted photon propagation in a backward direction. The predicted effect may be of interest for both production of quasimonochromatic intensive x-ray beams and diagnostics of solid structure [12, 18]. The strong modification of the density effect, as applied to the resulting coherent part of PB from a polycrystal, is demonstrated as well. The relativistic system of units $\hbar = c = 1$ is used in the paper.

2. The emission spectral-angular distribution

Let us consider properties of PB from relativistic electrons moving in a solid target. Starting from Maxwell's equations

$$(k^2 - \omega^2)\mathbf{E}_{\omega\mathbf{k}} - \mathbf{k}(\mathbf{k}\cdot\mathbf{E}_{\omega\mathbf{k}}) = 4\pi i\omega\mathbf{J}_{\omega\mathbf{k}} + \frac{i\omega e}{2\pi^2}\mathbf{V}\delta(\omega - \mathbf{k}\cdot\mathbf{V}), \tag{1}$$

for the Fourier transform of electric field $\mathbf{E}_{\omega\mathbf{k}} = (2\pi)^{-4}\int \mathrm{d}^3r\,\mathrm{d}t\,\mathrm{e}^{i\omega t - i\mathbf{kr}}\mathbf{E}(\mathbf{r}, t)$ we will elucidate the influence of inter-atomic correlations in the target on the PB yield ($\mathbf{V}$ in equation (1) is the velocity of an incident electron). Such correlations are described by the Fourier transform of the induced electron current density $\mathbf{J}_{\omega\mathbf{k}} = (2\pi)^{-4}\int \mathrm{d}t\,\mathrm{d}^3r\mathbf{J}(\mathbf{r}, t)\,\mathrm{e}^{i\omega t - i\mathbf{kr}}$, where $\mathbf{J}(\mathbf{r}, t)$ is determined by the averaging of the current density operator

$$\hat{\mathbf{J}} = \frac{e}{2m}\sum_{\alpha}[(\mathbf{p}_\alpha - e\mathbf{A})\delta(\mathbf{r} - \mathbf{r}_\alpha) + \delta(\mathbf{r} - \mathbf{r}_\alpha)(\mathbf{p}_\alpha - e\mathbf{A})], \tag{2}$$

over atomic wavefunctions calculated in first order in $\mathbf{E}(\mathbf{r}, t)$. The sum in (2) is taken over all the target's electrons, $\mathbf{p}_\alpha$ is the operator of the αth electron momentum, $\mathbf{r}_\alpha$ is its coordinate and $\mathbf{A}$ is the vector potential of an excited electromagnetic field; it is assumed that wavefunctions of different atoms do not overlap.

The expression for $\mathbf{J}_{\omega\mathbf{k}}$ following from (2) has the form

$$J_{\omega\mathbf{k},l} = \sum_p \int \mathrm{d}^3k' G_{lp}(\mathbf{k}, \mathbf{k}')E_{\omega\mathbf{k}',p}, \tag{3}$$

where the tensor $G_{lp}(\mathbf{k}, \mathbf{k}')$ presented in [19, 20] is rather complicated. In the frequency range $I \ll \omega \ll m$ of interest to us, where the Thomson scattering dominates (I is the average

ionization potential of an atom, m is the electron mass) the quantity $G_{lp}(\mathbf{k}, \mathbf{k}')$, is reduced to a simple form

$$4\pi \mathrm{i}\omega G_{lp}(\mathbf{k}, \mathbf{k}') = -\delta_{lp}\frac{e^2}{2\pi^2 m}\sum_j \mathrm{e}^{\mathrm{i}(\mathbf{k}'-\mathbf{k})\mathbf{r}_j} F(\mathbf{k}-\mathbf{k}') \equiv -\delta_{lp} G(\mathbf{k}'-\mathbf{k}), \tag{4}$$

where $\mathbf{r}_j$ is the coordinate of the jth atom in the target and $F(\mathbf{k}-\mathbf{k}')$ is the form factor of an atom.

Equations (1), (3) and (4) give a traditional description of x-ray elastic scattering for x-ray diffraction theory [21]. This description is most suitable for solid targets consisting of relatively light atoms ($Z < 20$) and for photon energy range 1–10 keV. Within the frame of approximation used, electrons of a single atom make a coherent contribution to the formation of the PB yield. On the other hand, a coherent contribution of all the target's atoms to the total PB yield depends strongly on the distribution of these atoms on their coordinates $\mathbf{r}_j$.

Substituting formulae (3) and (4) into equation (1) and separating the function $G(\mathbf{k}'-\mathbf{k})$ into average and accidental components

$$\begin{aligned} G(\mathbf{k}'-\mathbf{k}) &\equiv \bar{G}(\mathbf{k}'-\mathbf{k}) + \tilde{G}(\mathbf{k}'-\mathbf{k}), \\ \bar{G}(\mathbf{k}'-\mathbf{k}) &= \langle G(\mathbf{k}'-\mathbf{k})\rangle = \omega_p^2 \delta(\mathbf{k}'-\mathbf{k}), \end{aligned} \tag{5}$$

one can put equation (1) in a more convenient form

$$(k^2 - \omega^2\varepsilon(\omega))\mathbf{E}_{\omega\mathbf{k}} + \int \mathrm{d}^3k' \tilde{G}(\mathbf{k}'-\mathbf{k})\left(\mathbf{E}_{\omega\mathbf{k}'} - \mathbf{k}\frac{\mathbf{k}\cdot\mathbf{E}_{\omega\mathbf{k}'}}{\omega^2\varepsilon(\omega)}\right) = \frac{\mathrm{i}\omega e}{2\pi^2}\left(\mathbf{V} - \frac{\mathbf{k}}{\omega\varepsilon(\omega)}\right)\delta(\omega - \mathbf{k}\cdot\mathbf{V}). \tag{6}$$

The brackets $\langle\,\rangle$ in (5) mean the averaging over coordinates of atoms $\mathbf{r}_\alpha$, $\omega_p = \sqrt{\frac{4\pi Z e^2 n_0}{m}}$ is the plasma frequency of the target, Z is the number of electrons in an atom, n_0 is the density of atoms and $\varepsilon(\omega) = 1 - \omega_p^2/\omega^2$ is the average dielectric permeability of the target, describing the influence of refractive properties of the target on PB characteristics (among other things, the density effect in PB is described by $\varepsilon(\omega)$). The approach used does not take into account the effect of a photoabsorption, but this defect may be eliminated on a phenomenological addition of the imaginary part to the dielectric permeability (it should be noted that the photoabsorption is not very substantial in the frequency range under consideration).

The solution of (6) obtained by the perturbation method in first order in $\tilde{G}$ has the following form:

$$\begin{aligned} \mathbf{E}_{\omega\mathbf{k}} = \mathbf{E}_{\omega\mathbf{k}}^{\mathrm{Coul}} + \mathbf{E}_{\omega\mathbf{k}}^{\mathrm{Rad}} &= \frac{\mathrm{i}\omega e}{2\pi^2}\left(\mathbf{V} - \frac{\mathbf{k}}{\omega\varepsilon(\omega)}\right)\frac{\delta(\omega - \mathbf{k}\cdot\mathbf{V})}{k^2 - \omega^2\varepsilon(\omega)} - \frac{\mathrm{i}\omega e}{2\pi^2}\frac{1}{k^2 - \omega^2\varepsilon(\omega)} \\ &\times \int \frac{\mathrm{d}^3k'}{k'^2 - \omega^2\varepsilon(\omega)}\tilde{G}(\mathbf{k}'-\mathbf{k})\left(\mathbf{V} - \frac{\mathbf{k}'}{\omega\varepsilon(\omega)} - \mathbf{k}\frac{\mathbf{k}\cdot\mathbf{V} - \mathbf{k}\cdot\mathbf{k}'/\omega\varepsilon(\omega)}{\omega^2\varepsilon(\omega)}\right) \\ &\times \delta(\omega - \mathbf{k}'\cdot\mathbf{V}), \end{aligned} \tag{7}$$

where the first term describes the projectile's Coulomb field and the last one corresponds to the PB field appearing due to the scattering of the above Coulomb field by heterogeneities of the target's electron density. Calculation of the Fourier integral $\mathbf{E}_\omega^{\mathrm{Rad}} = \int \mathrm{d}^3k\, \mathrm{e}^{\mathrm{i}\mathbf{k}\mathbf{r}}\mathbf{E}_{\omega\mathbf{k}}^{\mathrm{Rad}} \to \mathbf{A}_\mathbf{n} \exp(\mathrm{i}\omega\sqrt{\varepsilon(\omega)}r)/r$ in a wave zone by the stationary phase method allows one to obtain the

following final expression for the emission amplitude $\mathbf{A_n}$:

$$\mathbf{A_n} = -\mathrm{i}\omega e \int \frac{\mathrm{d}^3k}{k^2 - \omega^2\varepsilon} \tilde{G}(\mathbf{k} - \omega\sqrt{\varepsilon}\mathbf{n}) \left(\mathbf{V} - \frac{\mathbf{k}}{\omega\varepsilon} - \mathbf{n}\left(\mathbf{n}\cdot\mathbf{V} - \frac{\mathbf{n}\cdot\mathbf{k}}{\omega\varepsilon} \right) \right) \delta(\omega - \mathbf{k}\cdot\mathbf{V}), \tag{8}$$

where $\mathbf{n}$ is the unit vector to the direction of emitted photon propagation.

The spectral-angular distribution of PB following from (8)

$$\begin{aligned} \omega \frac{\mathrm{d}N}{\mathrm{d}\omega\,\mathrm{d}\Omega} = e^2\omega^2 \int & \frac{\mathrm{d}^3k'}{k'^2 + 2\omega\sqrt{\varepsilon}\mathbf{n}\cdot\mathbf{k}'} \frac{\mathrm{d}^3k''}{k''^2 + 2\omega\sqrt{\varepsilon}\mathbf{n}\cdot\mathbf{k}''} \langle \tilde{G}(\mathbf{k}')\tilde{G}^*(\mathbf{k}'') \rangle \\ & \times \left[\mathbf{V} - \frac{\mathbf{k}'}{\omega\varepsilon} - \mathbf{n}\left(\mathbf{n}\cdot\mathbf{V} - \frac{\mathbf{n}\cdot\mathbf{k}'}{\omega\varepsilon} \right) \right] \left[\mathbf{V} - \frac{\mathbf{k}''}{\omega\varepsilon} - \mathbf{n}\left(\mathbf{n}\cdot\mathbf{V} - \frac{\mathbf{n}\cdot\mathbf{k}''}{\omega\varepsilon} \right) \right] \\ & \times \delta[\omega(1 - \sqrt{\varepsilon}\mathbf{n}\cdot\mathbf{V}) - \mathbf{k}'\cdot\mathbf{V}]\delta[\omega(1 - \sqrt{\varepsilon}\mathbf{n}\cdot\mathbf{V}) - \mathbf{k}''\cdot\mathbf{V}], \end{aligned} \tag{9}$$

depends strongly on inter-atomic correlations in the target, described by the correlator $\langle \tilde{G}(\mathbf{k}')\tilde{G}^*(\mathbf{k}'') \rangle$. In order to show the influence of such correlations on PB properties let us calculate the correlator assuming that the target consists of accidentally oriented perfect microcrystals containing a high enough number of atoms, so that the process of the projectile's Coulomb field scattering by a single microcrystal is close to Bragg scattering by an unbounded monocrystal. As this takes place, radiation from different microcrystals generally does not interfere because of the very small angular width of the Bragg diffraction mechanism, which is why each microcrystal dissipates the projectile Coulomb field independently. Under the conditions under consideration the procedure of averaging in $\langle \tilde{G}(\mathbf{k}')\tilde{G}^*(\mathbf{k}'') \rangle$ reduces to a well-known averaging of the sum $\sum_j \sum_l \mathrm{e}^{\mathrm{i}\mathbf{k}'\mathbf{r}_j - i\mathbf{k}''\mathbf{r}_l}$ for a monocrystal [15] (it is believed that $\mathbf{r}_\alpha = \mathbf{r}_n + \mathbf{r}_{nl} + \mathbf{u}_{nl}$, where $\mathbf{r}_n$ is the coordinate of the nth elementary cell in a monocrystal, $\mathbf{r}_{nl}$ is the equilibrium position of the lth atom in the nth cell and $\mathbf{u}_{nl}$ is the thermal displacement of the nlth atom) attended by the averaging over monocrystal orientations. The result of averaging of the correlator has the form

$$\begin{aligned} \langle \tilde{G}(\mathbf{k}')\tilde{G}^*(\mathbf{k}") \rangle = \frac{2e^4 n_a}{\pi m^2} \delta(\mathbf{k}' - \mathbf{k}") \Bigg[& (2\pi)^3 n_a \sum_{\mathbf{g}}{}' |S(\mathbf{g})|^2 F^2(g)\, \mathrm{e}^{-g^2U_\mathrm{T}^2} \frac{1}{4\pi g^2} \delta(k' - g) \\ & + F^2(k')\left(1 - \mathrm{e}^{-k'^2U_\mathrm{T}^2}\right) \Bigg], \end{aligned} \tag{10}$$

where n_a is the density of atoms, $S(\mathbf{g}) = \frac{1}{N_0}\sum_{j=1}^{N_0} \mathrm{e}^{\mathrm{i}\mathbf{g}\cdot\mathbf{r}_j}$ is the structure factor of an elementary cell containing N_0 atoms, U_T is the mean square amplitude of thermal vibrations of an atom and $\mathbf{g}$ is the reciprocal lattice vector. The first and second terms in square brackets describe collective and individual contributions of atoms to the PB yield respectively.

Formulae (9) and (10) giving a full description of collective effects in PB will be used in subsequent analysis.

3. Coherent peaks in the PB spectrum

Embarking on an analysis of PB properties, let us point out the effect of incoherent PB suppression in the case of a solid polycrystalline target under consideration. Indeed, the form factor $F(\mathbf{g})$ distinguishes substantially from zero in the range $k' \leqslant 1/R$ (R is the screening radius in the Fermi–Thomas atom model). Because of this, the coefficient $1 - \mathrm{e}^{-k'^2U_\mathrm{T}^2}$ in (8) is very small $\left(1 - \mathrm{e}^{-k'^2U_\mathrm{T}^2} \approx k'^2U_\mathrm{T}^2 \leqslant U_\mathrm{T}^2/R^2 \sim 10^{-2}\right)$. The effect under consideration is analogous to that in the physics of ordinary bremsstrahlung from relativistic electrons moving in a crystalline or polycrystalline target, but in contrast with a total suppression of the incoherent part of PB incoherent bremsstrahlung decreases by only 10%

[15]. This sharp distinction is caused by the difference between effective impact parameters b for PB and bremsstrahlung ($b \sim R$ and $b \sim 1/m$ respectively).

The final formula for the spectral-angular distribution of the coherent part of PB follows from (9) and (10) in the form

$$\omega\frac{\mathrm{d}N}{\mathrm{d}t\,\mathrm{d}\omega\,\mathrm{d}\Omega} = \sum_{\mathbf{g}}{}' \omega\frac{\mathrm{d}N_{\mathbf{g}}}{\mathrm{d}t\,\mathrm{d}\omega\,\mathrm{d}\Omega}, \qquad \omega\frac{\mathrm{d}N_{\mathbf{g}}}{\mathrm{d}t\,\mathrm{d}\omega\,\mathrm{d}\Omega} = A_{\mathbf{g}}\Phi_{\mathbf{g}}(\omega,\theta),$$

$$A_{\mathbf{g}} = \frac{\pi e^6 n_a^2}{m^2 g^3}|S(\mathbf{g})|^2 F^2(g)\,\mathrm{e}^{-g^2U_{\mathrm{T}}^2},$$

$$\Phi_{\mathbf{g}} = \frac{g^2}{\omega^2}\sigma\left(\frac{gV}{1-\sqrt{\varepsilon}V\cos\theta}-\omega\right)$$
$$\times\left\{2\frac{1+2\frac{\omega^2}{g^2V^2}\varepsilon^{\frac{3}{2}}V^3\cos\theta}{\sqrt{\left(1-2\frac{\omega^2}{g^2V^2}(1-\sqrt{\varepsilon}V\cos\theta)\right)^2+4\frac{\omega^2}{g^2V^2}(1-\varepsilon V^2)\left(1-\frac{\omega^2}{g^2V^2}(1-\sqrt{\varepsilon}V\cos\theta)^2\right)}}\right.$$
$$-1-\left(1+2\frac{\omega^2}{g^2V^2}\sqrt{\varepsilon}V\cos\theta(1-\sqrt{\varepsilon}V\cos\theta)\right)$$
$$\left.\times\frac{\left(1-2\frac{\omega^2}{g^2V^2}\varepsilon V^2(1-\sqrt{\varepsilon}V\cos\theta)\right)^2+4\frac{\omega^4}{g^4V^4}\varepsilon^2V^4(1-\varepsilon V^2)}{\left[\left(1-2\frac{\omega^2}{g^2V^2}(1-\sqrt{\varepsilon}V\cos\theta)\right)^2+4\frac{\omega^2}{g^2V^2}(1-\varepsilon V^2)\left(1-\frac{\omega^2}{g^2V^2}(1-\sqrt{\varepsilon}V\cos\theta)^2\right)\right]^{\frac{3}{2}}}\right\}, \tag{11}$$

where $\mathbf{n}\cdot\mathbf{V} = V\cos\theta$, $\sigma(x) = 1$ if $x > 0$ and $\sigma(x) = 0$ if $x < 0$.

Expression (11) demonstrates three distinctive properties of relativistic electron PB additional to the above suppression of the incoherent part of PB in a solid polycrystalline target as compared with that in an amorphous one. There are occurrences of strong peaks in a PB spectrum realizing in the vicinity of Bragg frequencies $\omega_g = gV/\sqrt{2(1-\sqrt{\varepsilon}V\cos\theta)} \approx g/2\sin(\theta/2)$, the existence of maximum frequency $\omega_{\max} = gV/(1-\sqrt{\varepsilon}V\cos\theta) \approx g/2\sin^2(\theta/2)$ for each g, the strong influence of the density effect on the coherent part of PB.

The manifestation of the above coherent peaks (the nature of these peaks is analogous to that of Debye–Scherrer peaks in the process of x-ray scattering in polycrystals) follows from (11) because of a small value of the coefficient $1-\varepsilon V^2 \simeq \gamma_*^{-2} = \gamma^{-2} + \omega_p^2/\omega^2 \ll 1$ in the denominators of this formula. It should be noted that the result (11) does not take into account a contribution of ordinary bremsstrahlung concentrated in the range of observation angles $\theta \leqslant \gamma_*^{-1}$. Let us consider the maximum of the spectral-angular distribution (11) for large observation angles $\theta \gg \gamma_*^{-1}$, where the PB contribution can dominate. In accordance with (11) the function $\Phi_{\mathbf{g}} \sim 1$ in the frequency range far from the vicinity of the Bragg frequency $\omega = \omega_g$. On the other hand, $\Phi_{\mathbf{g}}(\omega_g)$ is determined by the formula

$$\Phi_{\mathbf{g}}(\omega_g) \simeq \frac{2\gamma_*\sin(\theta/2)}{\sqrt{\cos^2(\theta/2)-\frac{1}{4}\gamma_*^{-2}\cos\theta}} \equiv \Phi_{\mathbf{g}}|_{\max}, \tag{12}$$

which shows the great enhancement of the PB yield under conditions of Bragg resonance [12, 18].

Now we should concentrate our attention on the new effect in PB following from formula (12) This formula predicts a substantial growth of PB spectral density for photons emitted in a backward direction. Indeed, the function $\Phi_{\mathbf{g}}(\omega_g)$ is proportional to γ_* for observation angles θ far from the value $\theta = \pi$. On the other hand, this function is proportional

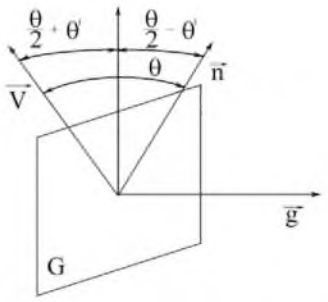

Figure 1. Geometry of the emission process. G is the reflecting crystallographic plane, $\mathbf{g}$ is the reciprocal lattice vector, $\mathbf{V}$ is the velocity of an emitting electron and $\mathbf{n}$ is the unit vector to the direction of emitted photon propagation.

to $\gamma_*^2 \gg \gamma_*$ if $\theta = \pi$. In addition to this, the spectral width of PB $\Delta\omega$ decreases in accordance with the formula

$$\frac{\Delta\omega}{\omega} \approx \frac{\sqrt{\cos^2(\theta/2) - \frac{1}{4}\gamma_*^{-2}\cos\theta}}{2\gamma_* \sin(\theta/2)}, \tag{13}$$

simultaneously with an increase in $\Phi_{\mathbf{g}}|_{\max}$, as the observation angle θ tends to π.

To explain results (12) and (13), let us consider the process of emission formation in greater detail. It is apparent that only microcrystals with crystallographic planes placed close to the Bragg resonance position relative to an incident electron beam can contribute substantially to the PB yield in the case of a polycrystalline target under consideration. The geometry of Bragg scattering of the projectile Coulomb field is shown in figure 1, where the angle θ' means the deviation from exact Bragg resonance. It is precisely this angle that determines PB spectral width for a fixed observation angle θ. Indeed, δ-functions $\delta(\omega(1 - \sqrt{\varepsilon}\mathbf{n}\cdot\mathbf{V}) - \mathbf{k}'\cdot\mathbf{V})$ and $\delta(k' - g)$ from equations (9) and (10) lead to the equation

$$\omega = \frac{\mathbf{g}\cdot\mathbf{V}}{1 - \sqrt{\varepsilon}\mathbf{n}\cdot\mathbf{V}} = \frac{gV\sin\left(\frac{\theta}{2} + \theta'\right)}{1 - \sqrt{\varepsilon}V\cos\theta} \approx \omega_g\left(1 + \theta'\mathrm{ctg}\left(\frac{\theta}{2}\right) - \frac{1}{2}\theta'^2\right). \tag{14}$$

Obviously, the coherent PB reflex generated by the Bragg scattering of projectile's Coulomb field on a fixed crystallographic plane is well-known parametric x-ray radiation (PXR) [15, 20, 22] (cross-section of coherent PB from a polycrystal results from the averaging of PXR cross-section over the angle θ'). Since a characteristic angular scale of the PXR reflex is about γ_*^{-1}, only crystallographic planes distributed within the range $-\gamma_*^{-1} \leqslant \theta' \leqslant \gamma_*^{-1}$ make the contribution to the PB yield from a polycrystal, so that the effective value of θ' in (14) is $\theta'_{\mathrm{eff}} \sim \gamma_*^{-1}$. The simple formula follows from (14)

$$\frac{\Delta\omega}{\omega} \sim \begin{cases} \gamma_*^{-1}\mathrm{ctg}\left(\dfrac{\theta}{2}\right) & \text{if} \quad \pi - \theta \gg \gamma_*^{-1} \\ \dfrac{1}{2}\gamma_*^{-2} & \text{if} \quad \theta = \pi \end{cases}, \tag{15}$$

which coincides practically with the corresponding limits of (13). Thus, the decrease of PB spectral width being discussed is of a geometrical origin.

Furthermore, the total PXR yield does not depend strongly on the value of the observation angle θ. From this fact, it is immediately inferred that a decrease in the PB spectral width must be accompanied by an increase in the amplitude of PB spectral distribution. One can easily see that this conclusion is in agreement with equations (12) and (13).

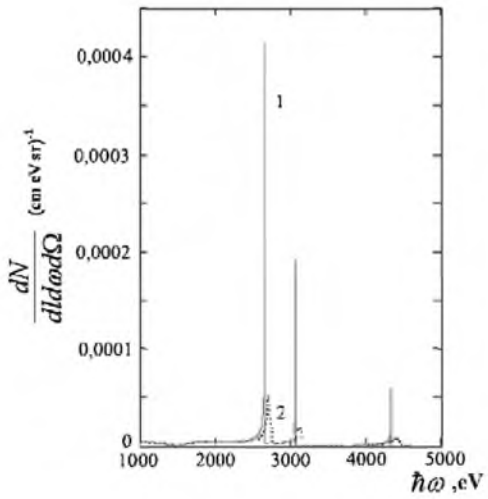

Figure 2. Manifestation of the anomalous peak in PB from the Al polycrystal. The energy of an emitting electron $\varepsilon = 15$ MeV; presented curves have been calculated for different values of the observation angle θ. $1 - \theta = 180^\circ$, $2 - \theta = 160^\circ$.

Returning to equation (12), which may be presented in the form

$$\Phi_{\mathbf{g}}|_{\max} \simeq \begin{cases} \dfrac{2\gamma \operatorname{tg}\left(\frac{\theta}{2}\right)}{\sqrt{1+\gamma^2/\gamma_c^2}} & \text{if} \quad \pi - \theta \gg \gamma_*^{-2} \\ \dfrac{4\gamma^2}{1+\gamma^2/\gamma_c^2} & \text{if} \quad \theta = \pi, \end{cases} \tag{16}$$

let us analyse an influence of the density effect on coherent PB. Here, the important quantity γ_c is determined by the formula

$$\gamma_c \simeq \frac{g}{2\omega_p \sin(\theta/2)}. \tag{17}$$

In accordance with (16) the PB spectral density is saturated as a function of γ in the range $\gamma > \gamma_c$, so that this inequality provides the condition of the density effect manifestation in PB from a polycrystalline target. The critical value of $\gamma = \gamma_c(\theta)$ decreases monotonically with an increasing observation angle θ. Because of this, the influence of the density effect on PB properties is substantial, primarily for large values of θ.

Anomalous peaks in PB are illustrated in figure 2. The curves presented in figure 2 have been calculated by formula (11) for fixed energy of emitting electron ($\gamma = 30$) and different values of the observation angle θ. Obviously, the enhancement of the PB spectral density due to the geometrical effect being considered is high enough. A strong asymmetry of PB photon flux emitted in the backward direction has engaged our attention. An explanation of this effect is very simple. The above formulae for the Bragg frequency ω_g and the maximum possible frequency $\omega_{\max}$ show that the difference $\omega_{\max} - \omega_g$ decreases when θ tends to π in accordance with the formula

$$\frac{\omega_{\max} - \omega_g}{\omega_{\max}} \simeq 1 - \sqrt{\sin^2(\theta/2) + \frac{1}{4}\gamma_*^{-2}\cos\theta} \to \frac{1}{8}\gamma_*^{-2} \ll 1. \tag{18}$$

Because of this anomalous PB spectral peak is bounded to the right of its maximum.

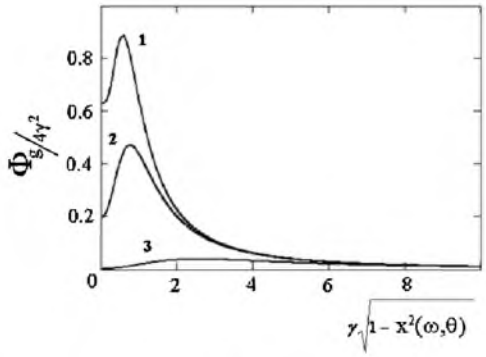

Figure 3. Influence of the density effect on the structure of the PB peak. The presented curves, describing the evolution of the spectrum of strongly collimated PB, have been calculated for $\gamma(\pi-\theta)=0,5$. 1: $\frac{\gamma}{\gamma_c}=0$, 1; 2: $\frac{\gamma}{\gamma_c}=1$; 3: $\frac{\gamma}{\gamma_c}=5$. The variables x and γ_c are determined in the text.

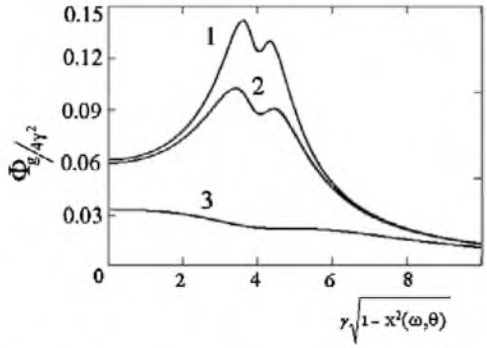

Figure 4. The same but for $\gamma(\pi-\theta)=8$.

Since the spectral width of an anomalous PB peak is very small, it is of interest to consider the form of this peak in more detail. In the vicinity of the points $\theta\approx\pi$, $\omega\approx\omega_{\max}$ where the anomalous peak is concentrated, the function Φ_g can be reduced to a more simple one

$$\frac{\Phi_g}{4\gamma^2}\simeq\frac{\left(\gamma^2(1-x^2)-\frac{1}{4}\gamma^2(\pi-\theta)^2\right)^2+\frac{1}{4}\left(1+\frac{\gamma^2\omega_p^2}{\omega^2}\right)\left(\gamma^2(1-x^2)+\frac{1}{4}\gamma^2(\pi-\theta)^2\right)}{\left(\left(\gamma^2(1-x^2)+\frac{1}{4}\left(1+\frac{\gamma^2\omega_p^2}{\omega^2}-\gamma^2(\pi-\theta)^2\right)\right)^2+\frac{1}{4}\left(1+\frac{\gamma^2\omega_p^2}{\omega^2}\right)\gamma^2(\pi-\theta)^2\right)^{\frac{3}{2}}},$$
$$x=\frac{\omega g}{V}(1+\sqrt{\varepsilon}V\cos(\pi-\theta))\simeq\frac{2\omega}{gV}\left(1-\frac{1}{4}(\gamma^{-2}+\frac{\omega_p^2}{\omega^2}+(\pi-\theta)^2)\right)\approx\frac{2\omega}{g}. \tag{19}$$

The obtained formula (19) allows us to trace an evolution of the PB spectrum as the observation angle θ recedes from π . Moreover, this formula is very convenient for estimations of an influence of the density effect on the PB anomalous peak. Such an influence is illustrated by the curves presented in figure 3. These curves calculated by (19) for the small deviation of θ from π demonstrate both the above-mentioned asymmetry of PB spectral distribution and substantial suppression of PB yield in the range of high enough emitting electron energies.

The curves presented in figure 4 have been calculated for a relatively large deviation of the observation angle θ from π. When figure 4 is compared with figure 3, it is apparent that

the difference between the maximum possible emitted photon energy and the Bragg frequency corresponding to the maximum of the PB spectral distribution increases as the angle θ moves away from π. In addition to this, the amplitude of the PB spectral distribution decreases simultaneously with an increase in the PB spectral width as the parameter $\gamma(\pi - \theta)$ increases in accordance with theoretical predictions. As in the case of small values of the parameter $\gamma(\pi - \theta)$, the PB yield is strongly suppressed by the density effect in the range of high enough electron energies.

Radical growth of the role of the density effect in PB from relativistic electrons moving through a polycrystalline structure as compared with that in an amorphous medium is caused by the coherent contribution of a target's atoms to the formation of the PB yield. As a consequence the transferred momentum $\mathbf{q}$ is fixed and equal to the reciprocal lattice vector $\mathbf{g}$, which is why the energy of emitted photons ω is approximately fixed as well ($\omega = \omega_g$). Under conditions of the density effect manifestation $\gamma\omega_p > \omega(\mathbf{q}) = \omega_g$ under consideration, most emitted photons are found to be suppressed. Physically, the coherent PB is formed in a large volume of the target (coherent volume inversely related to the transferred momentum and related to γ^2). Saturation of the transverse scale of the Coulomb field associated with an emitting electron due to the density effect terminates in the failure of phase relations between elementary waves emitted on different atoms arranged in the coherent volume and hence suppresses the yield of coherent PB.

4. Conclusions

In accordance with the performed analysis the spectral-angular distribution of a coherent PB peak from relativistic electrons moving through a solid polycrystalline target is proportional to the energy of an emitting electron in a wide region of observation angles, exclusive of the narrow vicinity of the backward direction.

In the above vicinity PB spectral intensity increases substantially and becomes proportional to the square of emitting electron energy. This effect has a geometrical nature (the number of microcrystals placed at the Bragg resonance position increases for photons emitted to the backward direction).

The intensity of anomalous PB peak being considered is saturated with an increase in the energy of an emitting electron due to the density effect.

It should be noted that the model of a polycrystalline target consisting of reasonably large microcrystals scattering a projectile Coulomb field by the Bragg mechanism was used in the performed calculations. Another model corresponding to PB from relativistic electrons moving in a small-grained medium has been considered in [23].

Acknowledgments

This work was accomplished in the context of the both the programme 'Advancement of the scientific potential of high education' by Russian Ministry of Education and Science (project RNP.2.1.1.3263) and Russian Foundation of Basic Research (grants: 06-02-16714 and 06-02-16942).

References

[1] Tystovich V and Oiringel I (eds) 1992 *Polarization Bremsstrahlung* (New York: Plenum)
[2] Korol A, Lyalin A and Solov'ev A 2004 *Polarization Bremsstrahlung* (St. Petersburg: St. PSPU Publishers) (In Russian)

[3] Astapenko V *et al* 2002 *Phys.-Usp.* **45** 149
[4] Korol A *et al* 2001 *J. Phys. B: At. Mol. Opt. Phys.* **34** 1589
[5] Korol A *et al* 2002 *Sov. Phys.—JETP* **94** 704
[6] Korol A *et al* 1996 *J. Phys. B: At. Mol. Opt. Phys.* **29** 617
[7] Ginzburg V and Tsytovich V 1979 *Phys. Rep.* **49** 1
[8] Amusia M and Korol A 1994 *Phys. Lett.* A **186** 230
[9] Gerchikov L and Solov'yov A 1997 *Zeit. Phys.* D **42** 279
[10] Connerade J and Solov'yov A 1996 *J. Phys. B: At. Mol. Opt. Phys.* **29** 3529
[11] Korol A and Solov'yov A 1997 *J. Phys. B: At. Mol. Opt. Phys.* **30** 1105
[12] Nasonov N 1998 *Nucl. Instrum. Methods* B **145** 19
[13] Nasonov N and Safronov A 1992 *Zh. Tech. Fiz.* **60** 1
[14] Astapenko V and Nasonov N 2006 *Zh. Eksp. Teor. Fiz.* **103** 553
[15] Ter-Mikaelian M 1972 *High Energy Electromagnetic Processes in Condensed Media* (New York: Wiley)
[16] Blazhevich S *et al* 1999 *Phys. Lett.* A **254** 230
[17] Takabayashi Y *et al* 2006 *Nucl. Instrum. Methods* B **243** 453
[18] Astapenko V *et al* 2006 *JETP Lett.* **84** 341
[19] Afanasev A and Kagan Yu 1968 *Acta Crystallogr.* A **24** 163
[20] Garibian G and Yang S 1972 *Zh. Eksp. Teor. Fiz.* **61** 930
[21] Battermann B and Cole H 1964 *Rev. Mod. Phys.* **36** 681
[22] Baryshevsky V and Feranchuk I 1971 *Zh. Eksp. Teor. Fiz.* **61** 944
[23] Nasonov N *et al* 2001 *Phys. At. Nuclei* **64** 966